Agricultural and Forest Meteorology 156 (2012) 75–84

Contents lists available at SciVerse ScienceDirect

Agricultural and Forest Meteorology

journal homepage: www.elsevier.com/locate/agrformet

Estimating the net ecosystem exchange for the major forests in the northern United States by integrating MODIS and AmeriFlux data

Xuguang Tang[a,b], Zongming Wang[a], Dianwei Liu[a,*], Kaishan Song[a], Mingming Jia[a], Zhangyu Dong[a], J. William Munger[c], David Y. Hollinger[d], Paul V. Bolstad[e], Allen H. Goldstein[f], Ankur R. Desai[g], Danilo Dragoni[h], Xiuping Liu[i]

[a] Northeast Institute of Geography and Agroecology, Chinese Academy of Sciences, Changchun 130012, China
[b] Graduate University of Chinese Academy of Sciences, Beijing 100049, China
[c] Department of Earth and Planetary Sciences, Harvard University, Cambridge, MA, USA
[d] US Forest Service, Northern Research Station, Durham, NH, USA
[e] Department of Forest Resources, University of Minnesota, St. Paul, MN, USA
[f] Department of Environmental Sciences, Policy, and Management, University of California, Berkeley, CA, USA
[g] Department of Atmospheric and Oceanic Sciences, University of Wisconsin, Madison, WI, USA
[h] Department of Geography, University of Indiana, Bloomington, IN, USA
[i] Key Laboratory of Agricultural Water Resources, Hebei Key Laboratory of Agricultural Water-Saving, Center for Agricultural Resources Research, Institute of Genetics and Developmental Biology, Chinese Academy of Sciences, Shijiazhuang 050021, China

ARTICLE INFO

Article history:
Received 21 April 2011
Received in revised form
21 December 2011
Accepted 3 January 2012

Keywords:
NEE
Eddy covariance
MODIS
EVI
LST
LSWI

ABSTRACT

The eddy covariance technique provides long-term continuous monitoring of site-specific net ecosystem exchange of CO_2 (NEE) across a large range of forest types. However, these NEE estimates only represent fluxes at the scale of the tower footprint and need to be scaled up to quantify NEE over regions or continents. In the present study, we expanded a method developed previously and generated a new NEE model exclusively based on the Moderate Resolution Imaging Spectroradiometer (MODIS) products, including enhanced vegetation index (EVI), land surface water index (LSWI), land surface temperature (LST) and Terra nighttime LST′. This method, in our previous research, provided substantially good predictions of NEE and well reflected the seasonal dynamics of the deciduous broadleaf forest at the Harvard forest site. Studying NEE of forests in the middle-latitude regions of the Northern Hemisphere is significant because it may help to understand the 'missing carbon sink' from terrestrial ecosystems. In this study we selected eight eddy flux sites to represent the major forest ecosystems in the northern United States. Compared with the model based on a single site, we also established the general models that apply to evergreen needleleaf forest (ENF) and deciduous broadleaf forest (DBF), respectively. The results showed that our simpler model based entirely on MODIS products promised well to estimate NEE by the eddy covariance technique. The modeled annual mean NEE from DBF deviated from the measured NEE by 44.4%, whereas the modeled NEE from ENF was extremely close to the measured NEE within 5.5%. In the end, we also validated both general models for ENF and DBF using independent flux sites. It demonstrated this method performed well for estimating NEE.

1. Introduction

Effects by forest ecosystem play a significant role in the global carbon cycle and help to mitigate atmospheric increases due to fossil fuel emissions (Schimel, 1995; Schimel et al., 2001; Alley et al., 2007). Net ecosystem carbon exchange (NEE), the balance between photosynthetic uptake and release of carbon dioxide by respiration from autotrophs and heterotrophs, represents the carbon sequestration between terrestrial ecosystems and the atmosphere during a given period. An accurate estimation of the spatial patterns and temporal dynamics of NEE in terrestrial ecosystems at the regional and global scale is of great interest to human society and is necessary for understanding the carbon cycle of the terrestrial biosphere (Xiao et al., 2010, 2011).

The temperate forests of the Northern Hemisphere have been identified as an important sink for storing atmospheric CO_2 with annual uptake values ranging between 70 and 870 $g\,C\,m^{-2}\,year^{-1}$ (Baldocchi et al., 2001; Law et al., 2002). Despite the consensus that the middle-latitude regions of the Northern Hemisphere are presently functioning as a carbon sink, the size and distribution of

* Corresponding author. Tel.: +86 43185542364; fax: +86 43185542299.
E-mail address: dianweiliu@gmail.com (D. Liu).

0168-1923/$ – see front matter © 2012 Elsevier B.V. All rights reserved.
doi:10.1016/j.agrformet.2012.01.003

the sink still remain uncertain (Pacala et al., 2001; Soccr, 2007). Traditionally, inventory studies of biomass and soil carbon are used to quantify NEE of an ecosystem over a specific period (Clark et al., 2001; Baldocchi, 2003). In recent years, with the development of the eddy covariance technique, which offers an alternative way to assess the ecosystem carbon exchange continuously and steadily for a long term, it has become possible to evaluate the carbon balance and its seasonal and annual variation of terrestrial ecosystems more precisely (Baldocchi, 2003). Furthermore, the carbon budgets and the effects of environmental controls for many forest types across the continent have also been quantified by this technique (Powell et al., 2006).

However, these NEE estimates only represent fluxes at the tower footprint scale, with longitudinal dimensions ranging from a hundred meters to several kilometers relying on homogeneous vegetation and fetch (Göckede et al., 2008). To quantify the net exchange of CO_2 over regions or continents, flux tower measurements from distributed points need to be scaled up to spatially continuous estimates (Xiao et al., 2010, 2011). Remotely sensed data from sensors such as MODIS are useful for monitoring the carbon flux, because reflectance can be converted into biophysically meaningful descriptors of the land surface (Yuan et al., 2006). Therefore, new approaches are critically needed to extend the role of field plots to capture regional variation and to bridge a major gap between field and satellite observations (Gregory et al., 2010). Earlier studies have shown good performance for integration of flux data with MODIS (Wylie et al., 2007; Yamaji et al., 2008; Xiao et al., 2010, 2011). Despite these efforts, most studies are still restricted to a specific biome, gross primary productivity (GPP), or single location like our own previous research on the deciduous broadleaf forest at the Harvard forest site (Wu et al., 2010; Tang et al., 2011).

Our objective is to develop a new method solely based on MODIS data for quantifying the spatial patterns and temporal changes in NEE of terrestrial ecosystems at large spatial scales. In previous research, we presented a model that provided good predictions of NEE and well reflected the seasonal dynamics of a deciduous broadleaf forest. Expanding on that work, here we encompassed the major forest types in the northern United States. We address the following questions:

(1) Can an approach that was developed at one site for deciduous, broadleaved forest be applied to other forest ecosystems?
(2) Based on multiple representative forest sites and the individual research, for each forest type, can we establish the general models that apply to evergreen needleleaf forest and deciduous broadleaf forest, respectively?

2. Materials and methods

2.1. Study sites description and distribution

The AmeriFlux network coordinates regional analysis of observations from eddy covariance flux towers across North America, Central America, and South America. This region covers a wide range of vegetation types including forests, shrublands, savannas, grasslands, and croplands. In the present study, we selected eight flux sites (conifer forest, 4; broadleaf forest, 4) to represent the major forest ecosystems in the northern United States (Fig. 1). Table 1 provides general information including site name, climate, stand age, vegetation characteristic, years of data available, and references for each flux site.

The four evergreen needleleaf forest sites represent considerable variation in location, climate, stand age, and species composition. The Blodgett forest (BF) is a young ponderosa pine forest in the Sierra Nevada Mountains of the western USA with moderate winters and relatively dry summers. The Niwot Ridge forest (NRF) is a subalpine temperate coniferous forest in the Rocky Mountains, with extreme winters and somewhat wetter summers than Blodgett. The Howland forest (HF) is located in a boreal-northern hardwood transition forest approximately 50 km north of Bangor, ME, USA. Forest composition is dominated by the conifers, red spruce (*Picea rubens* Sarg., 44% of basal area) and eastern hemlock (*Tsuga canadensis* (L.) Carriere, 26%) with lesser quantities of other conifers (21%) and hardwoods (primarily red maple, *Acer rubrum* L., and paper birch, *Betula papyrifera* Marsh., totaling 8% of basal area). The Metolius Intermediate Pine site (Me2) is located in the semi-arid region of Central Oregon. The local climate is typical of warm dry summers and cool wet winters. Most precipitation falls between October and June, accounting for approximately 97% of annual rainfall. The overstory is almost exclusively composed of ponderosa pine trees (*Pinus ponderosa* Doug. Ex P. Laws) with a few scattered incense cedars (*Calocedrus decurrens* (Torr.) Florin). The understory is sparse and primarily composed of bitterbrush (*Purshia tridentate* (Push) DC) and Manzanita (*Arctostaphylos patula* Greene). The four deciduous forest sites are characteristic of the eastern deciduous forests of North America, and represent a range of annual temperature regimes. The Morgan Monroe State forest (MMS) in Indiana is the warmest site and the Willow Creek (WC) in Wisconsin is the coldest (Cook et al., 2004). The Harvard tower is located in a mixed temperate forest, approximately 110 km west of Boston, MA, USA. Forest composition is dominated by deciduous species, including red oak (*Quercus rubra* L.; 36% of basal area) and red maple (22%), with lesser quantities of other hardwoods, including black oak (*Quercus velutina* Lam.), white oak (*Quercus alba* L.), and yellow birch (*Betula alleghaniensis* Britton) covering 14% of basal area. The University of Michigan Biological Station (UMBS) site is located within a protected forest owned by the University of Michigan. Bigtooth aspen (*Populus grandidentata* Michx.) and trembling aspen (*Populus tremuloides* Michx.) dominate within a 1 km radius of the eddy-covariance tower, but with significant representation by red oak, beech (*Fagus grandifolia* Ehrh.), sugar maple, white pine, and hemlock as well. The understory is dominated by bracken fern (*Pteridium aquilinum* L.) and saplings of red maple, red oak, beech, and white pine. All deciduous forest sites experience high amounts of summer rainfall (typically between 225 and 300 mm). Among the eight AmeriFlux sites, Me2 and UMBS are used as the independent sites to validate the developed general models for evergreen needleleaf forest and deciduous broadleaf forest, respectively.

2.2. MODIS products and processing

Optical remote sensing systems measure the surface reflectance, the fraction of solar energy that is reflected by the earth's surface. For a given wavelength, different vegetation types may have different reflectance. The reflectance also depends on wavelength region, biophysical properties (e.g., biomass, leaf area, and stand age), soil moisture and sun-sensor geometry. Therefore, reflectance values from MODIS can provide useful information for NEE estimation. This temperature and greenness (TG) model includes two vegetation indices as input data: EVI and LSWI. EVI directly adjusts the reflectance in the red band as a function of reflectance in the blue band, accounting for residual atmospheric contamination, variable soil and canopy background reflectance. Huete et al. (2002) have developed a global EVI product from MODIS data for the period 2000 to present, defined as

$$\mathrm{EVI} = 2.5\frac{\rho_{\mathrm{nir}} - \rho_{\mathrm{red}}}{\rho_{\mathrm{nir}} + (6\rho_{\mathrm{red}} - 7.5\rho_{\mathrm{blue}}) + 1} \quad (1)$$

where ρ_{nir}, ρ_{red}, and ρ_{blue} are the spectral reflectance in MODIS bands 2, 1 and 3, respectively.

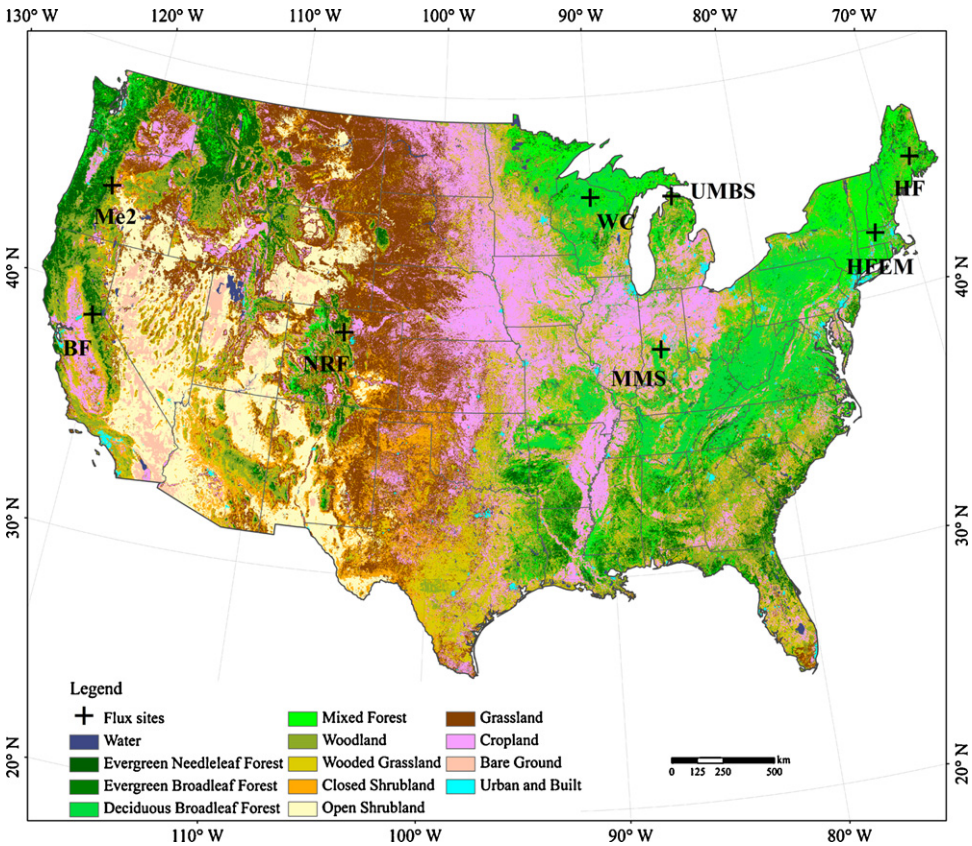

Fig. 1. Location and spatial distribution of the AmeriFlux sites used in the present study. The base map is derived from AVHRR 1 km land-cover map. Symbols indicate the location of the sites. The full site names are as follows: BF, Blodgett forest; HF, Howland forest; NRF, Niwot Ridge forest; MMS, Morgan Monroe State forest; HFEM, Harvard forest site; WC, Willow Creek; Me2, Metolius Intermediate Pine; UMBS, University of Michigan Biological Station.

As the shortwave infrared (SWIR) spectral band is sensitive to vegetation water content and soil moisture, a combination of NIR and SWIR bands have been used to derive water-sensitive vegetation indices (Ceccato et al., 2002). Gao (1996) developed the LSWI from satellite data to measure vegetation liquid water:

$$\mathrm{LSWI} = \frac{\rho_{\mathrm{nir}} - \rho_{\mathrm{swir}}}{\rho_{\mathrm{nir}} + \rho_{\mathrm{swir}}} \tag{2}$$

where ρ_{swir} is the reflectance in MODIS band 6. LSWI was shown to strongly correlate with leaf water content (equivalent water thickness, g H_2O m^{-2}) (Jackson et al., 2004) and soil moisture overtime (Fensholt and Sandholt, 2003). The other explanatory variable is LST. The LST derived from MODIS is a measure of the surface temperature. A few studies have demonstrated that the satellite-derived LST was strongly correlated with ecosystem respiration (R_e) as both autotrophic and heterotrophic respirations are significantly affected by air/surface temperature (Rahman et al., 2005; Sims et al., 2008; Schubert et al., 2010).

Therefore, we selected EVI, LSWI and LST (including Terra daytime LST and Terra nighttime LST′) as the explanatory variables for NEE estimation. All these variables were derived from MODIS data, which also avoided the complications and difficulties associated with merging disparate data sources. The 8-day Land Surface Reflectance (MOD09A1, with resolution of 500 m) and LST data (MOD11A2, with resolution of 1 km) were obtained from the 7 km × 7 km subsets of MODIS products available at the Oak Ridge National Laboratory's Distributed Active Archive Center web site (http://www.modis.ornl.gov/modis/index.cfm). The version of MODIS data is collection 5. Average values for the central 3 km × 3 km area were extracted within the 7 km × 7 km cutouts to better represent the flux tower footprint (Rahman et al., 2005). The reflectance values of these four spectral bands – blue, red, near infrared (841–875 nm), and shortwave infrared (1628–1652 nm) in 2001–2004 were used to calculate EVI and LSWI. At each time step, we averaged the values of each variable using the pixels with good quality within the area to represent the values at the flux site. If none of the values within the 3 km × 3 km area was of good quality, we treated the period as missing (Schubert et al., 2010).

2.3. Eddy covariance data

Measurements of CO_2 exchange between the vegetation and atmosphere for each site were made with the eddy covariance technique. This direct, long-term measurement of carbon fluxes offers the possibility to assess the carbon sequestration rates of forests and of different land-uses on a local scale. This technique can also provide a better understanding of the vulnerability of the carbon balance of ecosystems to climate variability, and can be used to validate ecosystem models, as well as to provide data for land surface exchange schemes in global models (Valentini et al., 2000). This is the flux that provides a measure of NEE, and if annually summed, provides a direct estimate of the annual ecosystem carbon balance excluding disturbances by harvest and fire that give rise to net biome productivity (Schulze and Heimann, 1998).

We used four-year eddy covariance measurements of NEE made at each site (http://public.ornl.gov/ameriflux/) (Table 1). Site-specific procedures, including quality control, flux corrections and data editing, are described elsewhere (Hollinger et al., 2004; Urbanski et al., 2007). The Level 4 product consists of two types of NEE data, including standardized (NEE_st) and original (NEE_or) NEE (AmeriFlux 2007). NEE_st was calculated using CO_2 flux estimated by the eddy covariance method, which includes summation

Table 1
Characteristics of the AmeriFlux tower sites used in the present study.

Name	Temperature (°C)	Precipitation (mm)	Elevation (m)	Stand age (yr)	Vegetation structure	Vegetation type	Years	References
BF	11.9	1416	1315	20	Mixed evergreen coniferous forest dominated by ponderosa pine	Evergreen needleleaf forest	2001–2004	Goldstein et al. (2000)
HF	6.1	990	60	110	Boreal-northern hardwood transitional forest consisting of hemlock–spruce–fir, aspen–birch, and hemlock–hardwood mixtures	Evergreen needleleaf forest	2001–2004	Hollinger et al. (2004)
NRF	1.5	692	3050	100	Subalpine coniferous forest dominated by subalpine, Engelmann spruce, and pine	Evergreen needleleaf forest	2001–2004	Monson et al. (2002)
MMS	10.8	1094	275	70	Mixed hardwood deciduous forest dominated by sugar maple, tulip poplar, sassafras, and oaks	Deciduous broadleaf forest	2001–2004	Schmid et al. (2000)
HFEM	6.5	1000	340	80	Temperate deciduous forest dominated by red oak, red maple, black birch, and white pine	Deciduous broadleaf forest	2001–2004	Urbanski et al. (2007)
WC	4.1	815	515	55–90	Temperate/boreal forest dominated by white ash, sugar maple, basswood, green ask, and red oak	Deciduous broadleaf forest	2001–2004	Desai et al. (2005)
Me2	7.6	540	1253	90	The surrounding overstory is dominantly ponderosa pine with scare incense cedar.	Evergreen needleleaf forest	2004	Thomas et al. (2009)
UMBS	6.2	750	234	80	Arboreal composition of the forest consists of mid-aged northern hardwoods, conifer understory, aspen, and old growth hemlock	Deciduous broadleaf forest	2004	Curtis et al. (2002)

BF, Blodgett forest; HF, Howland forest; NRF, Niwot Ridge forest; MMS, Morgan Monroe State forest; HFEM, Harvard forest site; WC, Willow Creek; Me2, Metolius Intermediate Pine; UMBS, University of Michigan Biological Station. Among the eight AmeriFlux sites, Me2 and UMBS are the independent sites for validation.

with CO_2 storage in the canopy air space that was obtained from the discrete approach (single point on the top of the tower) for all the sites, whereas NEE_or was calculated using the storage obtained from within canopy CO_2 profile measurements in relatively tall forest canopies or from the discrete approach. The average data coverage during a year is only 65% due to system failures or data rejection, and therefore robust and consistent gap filling methods are required for data set completion (Falge et al., 2001).

Both NEE_st and NEE_or were filled using the Marginal Distribution Sampling (MDS) method and the Artificial Neural Network (ANN) method. The ANN method is generally, if only slightly, superior to the MDS method (Papale and Valentini, 2003; Reichstein et al., 2005). Therefore, we used the gap-filled NEE data based on the ANN method. For each site, if the percentage of the remaining missing values for NEE_st was lower than that for NEE_or, we selected NEE_st; otherwise, we used NEE_or. In this product, negative sign denotes carbon uptake, and positive sign denotes carbon release (Xiao et al., 2011).

The Level 4 product consists of NEE data with four different time steps, including half-hourly, daily, weekly (8-day), and monthly. We used weekly NEE data (g C m^{-2} day^{-1}) to match the composting intervals of MODIS products. Moreover, the average NEE over such a period was shown to largely reduce micrometeorological sampling errors, with the remaining spatial variability representing variation in ecosystem attributes (Oren et al., 2006; Wang et al., 2010), here accounted for by data from MODIS.

3. Results and discussion

3.1. Model development

The development of our predictive model has been fully described by Tang et al. (2011). Here, we briefly summarize the approach. We developed a predictive NEE model by integrating the site-specific MODIS products and AmeriFlux data. The explanatory variables included EVI, daytime and nighttime LST, and LSWI; the target variable was NEE. We split the site-level data set into a training set (2001–2003) and a validation set (2004). After analyzing the Pearson correlation coefficients between these parameters and the observed NEE (Table 2), we used multiple linear regression method to select the model with the maximum coefficient of determination (R^2) and the minimum root mean square error (*RMSE*) to estimate NEE (Table 3). Based on multiple representative forest sites and the individual research, for each forest type, we also tried to establish the general models that apply to evergreen needleleaf forest and deciduous broadleaf forest, respectively.

3.2. NEE assessment by the temperature and greenness (TG) model

The TG model was run at 8-day time scale using the site-specific data of EVI, daytime and nighttime LST′, and LSWI to predict NEE for each flux site or forest type, as shown in Table 3. The model performance was then evaluated using scatter plots (Fig. 2) of predicted

Table 2
Correlation coefficients between NEE of each eddy covariance flux site or forest type and the corresponding MODIS products.[a]

	BF	HF	NRF	MMS	HFEM	WC	ENF	DBF
EVI	−0.028	−0.457	0.06	−0.923	−0.911	−0.916	−0.288	−0.877
LST	−0.642	−0.703	−0.644	−0.579	−0.663	−0.626	−0.692	−0.597
LST′	−0.578	−0.626	−0.635	−0.715	−0.751	−0.693	−0.637	−0.68
LSWI	0.615	0.533	0.714	−0.842	−0.484	−0.463	0.561	−0.57

[a] All MODIS products including EVI, LST, LST′ and LSWI are the average values for the 3 km × 3 km area centered on the tower. The full names of the abbreviations are given in Table 1. ENF and DBF refer to evergreen needleleaf forest and deciduous broadleaf forest, respectively.

versus measured NEE and the seasonal variations (Fig. 3) between them in 2004.

For the evergreen needleleaf forest sites, generally the predicted NEE by the TG model captured the broad trends of NEE from the flux site. They also showed a good agreement as regards seasonal dynamics (Figs. 2 and 3). However, this model significantly underestimated the photosynthetic activity by 1–1.5 g C m^{-2} day^{-1} in the summertime. The scatter plots showed that the residuals were not randomly distributed. In absolute magnitude, low NEE values were generally in accordance with low prediction errors, whereas high NEE values were greatly underestimated. This suggests that the uncertainties of carbon flux measurements are directly proportional to the magnitude of the fluxes. The general model of the three sites predicted NEE well with R^2 of 0.670 and *RMSE* of 0.603. Fig. 3 also showed that the model could not capture exceptionally high NEE values representing large carbon uptake. Particularly for some sites, such as the Blodgett forest (BF) and the Niwot Ridge forest (NRF), generally the predicted NEE varied more smoothly than the measured NEE.

The TG model provided better estimates of NEE for the deciduous broadleaf forest sites than for the conifer forest. Figs. 2 and 3 indicated that predicted NEE agreed reasonably well with observed NEE and captured most features of 8-day variability throughout the period of 2004. The validation points of estimated and measured NEE are distributed closely around the 1:1 line and the Pearson correlation coefficients of all the three deciduous forest sites were larger than 0.93. This result was very encouraging. However, when the relationship between measured and predicted NEE by the general model of the deciduous-dominated forest was examined, we found it overestimated NEE in most weekly periods (Fig. 2, DBF and Fig. 4, DBF). In the meantime, this model underestimated the carbon uptake in the peak growing season greatly as the same as evergreen needleleaf forest sites.

We averaged the estimated and measured 8-day NEE for each flux site and examined the relationship between them across the major forest types (Fig. 4). The TG model predicted NEE well at the site level. Overall, in absolute magnitude, the model underestimated NEE except that for the Willow Creek (WC) which was slightly larger than the observed. However, all the sites showed as carbon sinks on an annual mean basis. Among the three conifer forests, the young Blodgett forest (BF) site sequestered the most CO_2 and the cold Niwot Ridge forest (NRF) sequestered the least. All the deciduous broadleaf forest sites absorbed CO_2 strongly. On the whole, the trend of the uncertainty of annual mean carbon estimation is as follows: HF > NRF > HFEM > BF > MMS > WC (Fig. 4). In addition, the general model predicted NEE at the biome level well except that large overestimation of annual mean carbon uptake and fairly constant underestimation of NEE during summer months for the deciduous broadleaf forest (DBF), the assessment of evergreen needleleaf forest (ENF) was rather coincident with measured NEE. The percentage deviations of the agreement between modeled and measured NEE for DBF and ENF were 44.4 and 5.5%, respectively.

3.3. Independent validation of the general models

To validate the effectiveness and applicability of the developed general models for evergreen needleleaf forest and deciduous broadleaf forest, we also introduced Me2 and UMBS as independent sites. The model performance was evaluated using the scatter plots of predicted versus measured NEE and the seasonal variations between them in 2004.

As shown in Fig. 5, for Me2, the general model of evergreen needleleaf forest promised well to estimate NEE and captured the broad trend of seasonal dynamics. Like other conifer forest sites, it overestimated carbon uptake in the earlier and later period of 2004, and also underestimated carbon sequestration in the summertime. However, as a whole, the general model assessed the annual mean NEE well, with the percentage of deviation being 21.7%. The general model of deciduous broadleaf forest provided better estimates of NEE for UMBS than for Me2 except exceptionally high NEE values representing large carbon uptake (Fig. 6). Overall, most scatter points of NEE were distributed around the 1:1 line and captured the broad trends throughout the whole year. The Pearson correlation coefficients of UMBS reached up to 0.88.

Our present study demonstrated that MODIS data have great potential for scaling up plot-level NEE data to regional scales across a variety of forest ecosystems. Owing to the transient carbon pools and associated heterotrophic respiration that are difficult to

Table 3
Establishment of the best temperature and greenness (TG) model or general model (GM) for NEE estimation of each site or forest type.[a]

Site/forest type	Fitting function	R^2	*RMSE*
BF	NEE = 7.708 − 0.132 × LST + 1.107 × LST′ − 3.655 × EVI + 1.765 × LSWI	0.449	1.165
HF	NEE = 9.777 − 0.113 × LST + 0.077 × LST′ − 1.301 × EVI + 2.618 × LSWI	0.554	0.911
NRF	NEE = 1.275 − 0.029 × LST + 0.02 × LST′ +3.328 × LSWI	0.523	0.695
MMS	NEE = −2.73 + 0.076 × LST − 0.053 × LST′ − 13.239 × EVI + 0.475 × LSWI	0.863	1.101
HFEM	NEE = 20.886 + 0.039 × LST − 0.091 × LST′ − 15.792 × EVI − 3.737 × LSWI	0.851	1.348
WC	NEE = 5.632 + 0.05 × LST − 0.058 × LST′ − 12.624 × EVI − 2.909 × LSWI	0.877	1.198
ENF	NEE = 12.471 − 0.089 × LST + 0.045 × LST′ − 3.325 × EVI + 1.934 × LSWI	0.525	0.991
DBF	NEE = 5.743 + 0.043 × LST − 0.049 × LST′ − 12.713 × EVI − 1.071 × LSWI	0.795	1.432

[a] The full names of each flux site or forest type are given in Tables 1 and 2.

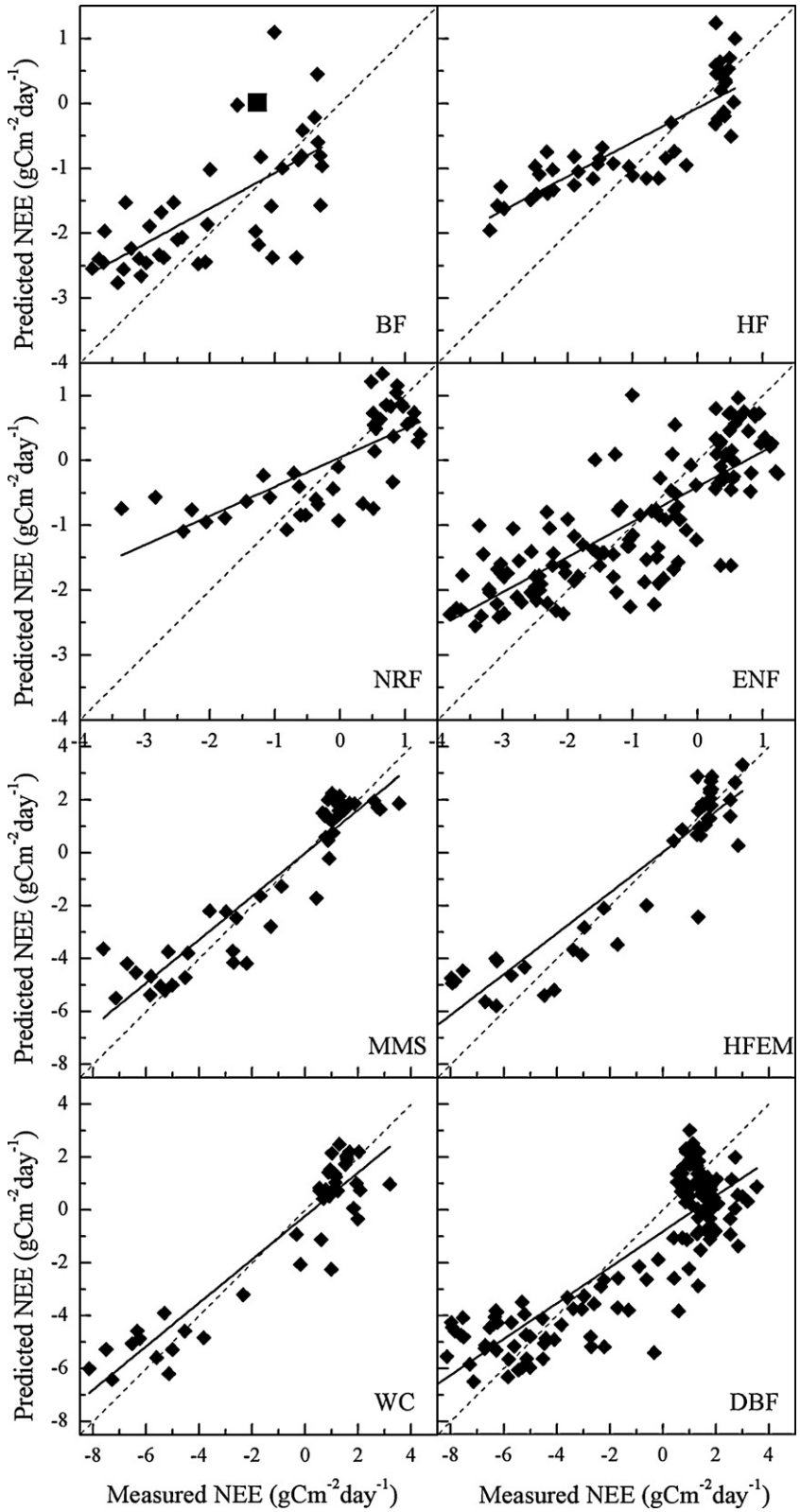

Fig. 2. Relationship between measured NEE and predicted NEE by the corresponding TG model or the general model (GM) for each flux site or forest type. The abbreviations of AmeriFlux sites or forest types are given in Table 1.

estimate, the determination of NEE is much more complicated than that of GPP (Running et al., 2004; Xiao et al., 2005; Li et al., 2007; Mahadevan et al., 2008). The performance of our general model for NEE estimation is encouraging given the diversity in climate, stand age, and community composition among the forest types.

3.4. Analysis of uncertainties

Despite the encouraging performance of our predictive model in estimating NEE and capturing the corresponding dynamics patterns of the major forest ecosystems in the northern United States,

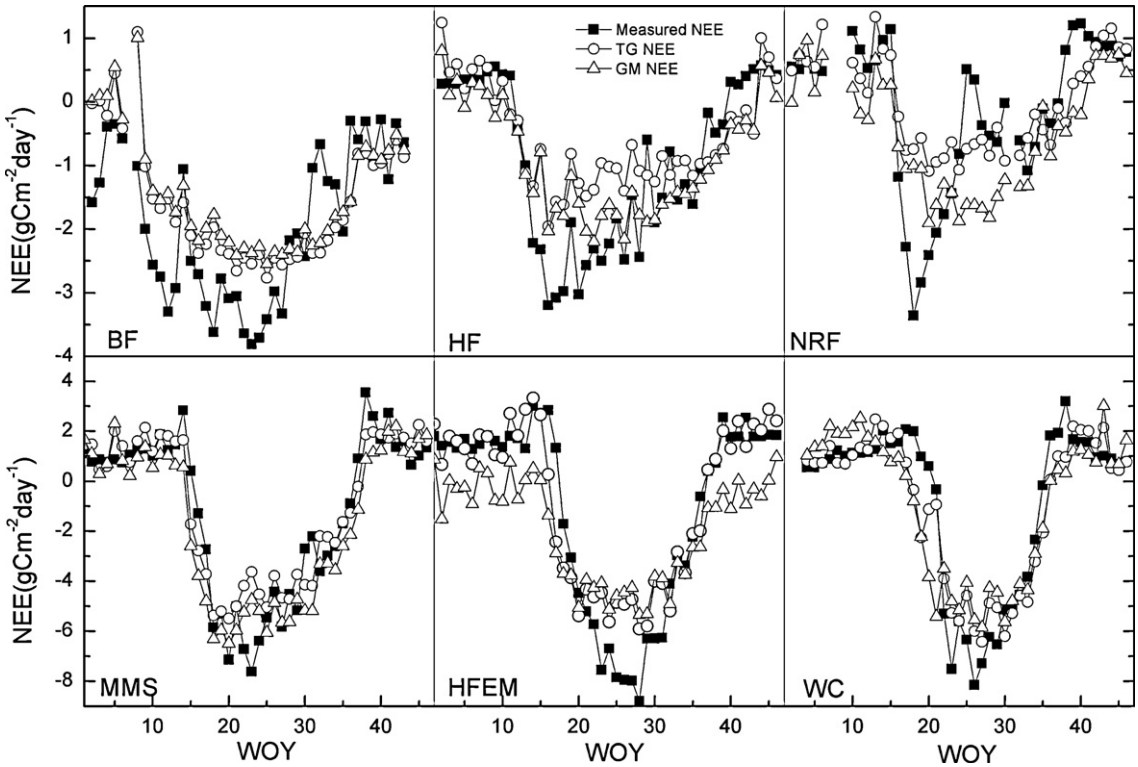

Fig. 3. Seasonal traces of measured and predicted 8-day NEE by the TG model or the general model (GM) for each flux site. For *x*-axis, the data refer to week of year (WOY) ranging from 1 to 46.

these NEE estimates still contain significant uncertainties and it is a long way from reliably estimating NEE.

There are several sources of uncertainty associated with the flux estimates: uncertainties in eddy flux measurements, uncertainties in input data, model structural uncertainty, and uncertainties arising from the representativeness of the limited AmeriFlux sites. The carbon flux measurements derived from the eddy flux towers contain significant uncertainties (Richardson et al., 2008), and the gap-filling techniques used to fill the data gaps introduced additional uncertainties of $\pm 25\,\mathrm{g\,C\,m^{-2}\,year^{-1}}$ (Moffat et al., 2007).

In this present study, we only selected EVI, LSWI and LST (including Terra daytime LST and Terra nighttime LST′) as the explanatory variables to estimate NEE. However, the factors controlling CO_2 exchange were complicated and these explanatory variables could not sufficiently account for NEE. NEE is the balance of canopy photosynthesis (GEE) and ecosystem respiration (R_e). GEE is controlled by canopy development as well as nutrient status, light, temperature, ambient humidity, CO_2 concentration, and soil moisture (Ruimy et al., 1996; Zhang et al., 2009). R_e includes contributions from autotrophs (vegetation) and heterotrophs (free living and fauna in the soil and symbiotic microorganisms) (Bowden et al., 1993; Ryan and Law, 2005; Zhou et al., 2010). Field studies of R_e have identified temperature, soil moisture, nutrient availability, stocks of living and dead biomass, ecosystem productivity, and seasonal carbon allocation as controlling factors (Boone et al., 1998; Wang et al., 2010). Thus, the use of subsets of these factors to drive functions that predict carbon fluxes, which is typical for the TG model, may limit the precision of estimation. We can also see that the importance of each influencing factor correlated with NEE varies greatly with forest types (Table 2). Due to the leaves of evergreen needleleaf forest are green around the whole year, EVI contributes least to NEE than the other remotely sensed variables. In addition, the inability of our model to account for transient carbon pools could introduce uncertainties to the NEE estimates. Thus, in future research, additional explanatory variables should be selected to better account for live and dead vegetation carbon pools, as well as other factors that influence the decomposition of woody detritus and soil respiration (Xiao et al., 2010; Zhu et al., 2010).

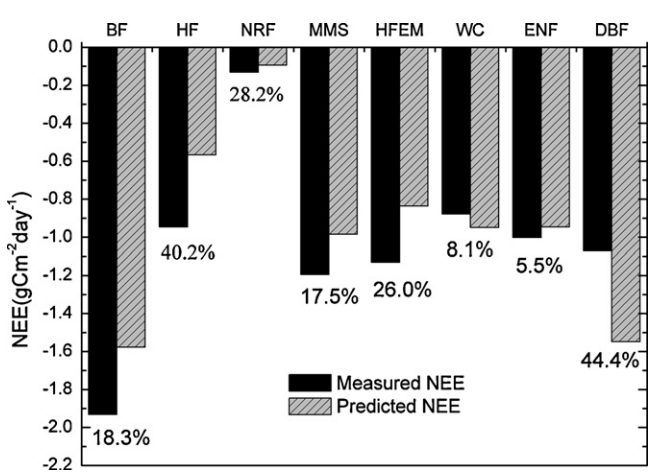

Fig. 4. Annual mean of measured and predicted NEE for each flux site or forest type in 2004. The unit is $\mathrm{g\,C\,m^{-2}\,day^{-1}}$. The temporal coverage of NEE data is provided in Fig. 2.

The representativeness of the limited AmeriFlux forest sites also presumably affected the estimates of carbon fluxes and the general applicability of our predictive model. The magnitude of net ecosystem productivity of an ecosystem depends on vegetation type, stand age, physical environment, latitude, and regional climate (Buchmann and Schulze, 1999; Valentini et al., 2000). Although in this study we selected eight flux sites to represent the major forest ecosystems that included most of the available sites in the network, some geographical regions, community composition, and different forest ages (young, middle aged and mature) of the same forest ecosystem are still underrepresented, which affect

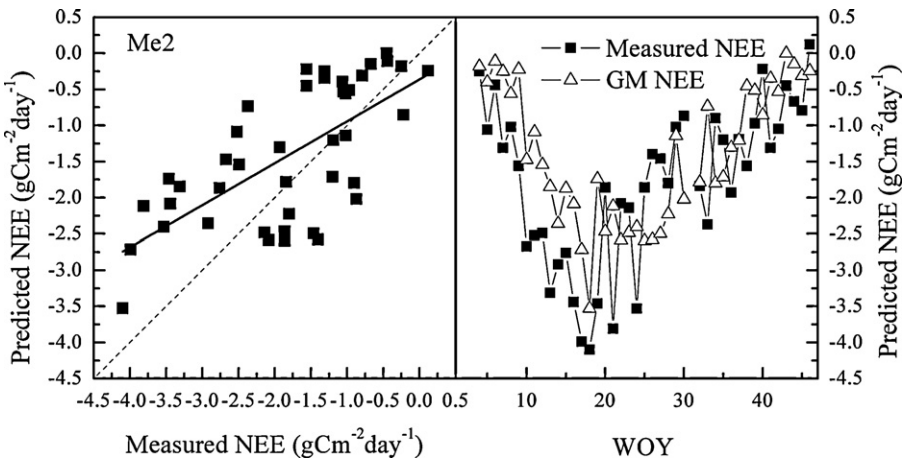

Fig. 5. Independent validation of the general model (GM) of evergreen needleleaf forest (ENF) – the scatter plots (left) and the seasonal dynamic (right) of measured and predicted NEE by the general model (GM) for Me2. WOY refers to week of year ranging from 1 to 46.

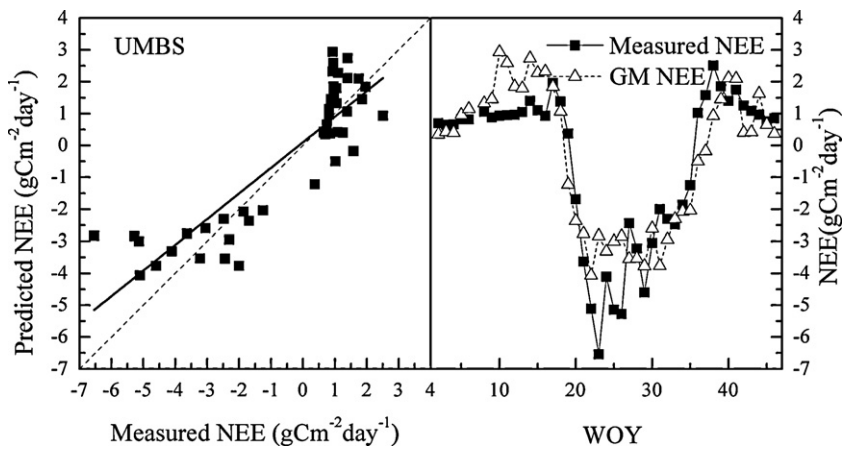

Fig. 6. Independent validation of the general model (GM) of deciduous broadleaf forest (DBF) – the scatter plots (left) and the seasonal dynamic (right) of measured and predicted NEE by the general model (GM) for UMBS. WOY refers to week of year ranging from 1 to 46.

the universality of the general models. Moreover, the flux sites of mixed broadleaf–conifer forest are very scarce. Thus, the current AmeriFlux network should be augmented by establishing more sites across a full range of forest types.

4. Conclusion

We combined plot-level MODIS and NEE data for the major forest types in the northern United States to develop a predictive NEE model using multiple linear regression approach. This continuous NEE estimation technique builds on our previous research. In the present study, we expanded the research objective from a single eddy covariance site to eight flux sites representing the major forest ecosystems in the northern United States. The model estimated NEE well for each 8-day period and generally captured the expected seasonal patterns of NEE. Therefore, our empirical approach has great potential for up-scaling NEE to large areas.

The AmeriFlux sites provide valuable measurements of ecosystem carbon exchange for examining terrestrial carbon dynamics and improving our understanding of the impacts of climate variability, disturbances, and management practices on terrestrial carbon cycling. Although the TG model works well for 8-day averaging periods, diurnal and day to day variation in NEE is still limited by the availability of satellite remote sensing at these timescales. Diurnal satellite data are not currently available and daily data are limited by cloud cover. However, our present study provides an alternative, independent, and novel approach for estimating the net ecosystem carbon exchange of the major forest ecosystems in the northern United States.

Acknowledgements

This study was supported by the Strategic Frontier Program of the Chinese Academy of Sciences (Grant no. XDA05050101) and the Knowledge Innovation Program of the Chinese Academy of Sciences (Grant no. KZCX2-YW-QN305). We thank the principal investigators and contributors of the MODIS products, the Distributed Active Archive Center of the Oak Ridge National Laboratory, and the Earth Observing System Data for making these MODIS data available. The towers were supported by Department of Energy Terrestrial Carbon Processes, NASA, DOE National Institute for Climate Change Research (NICCR), and the USDA. We also thank those involved in the maintenance, operation and collection of all the sites of the AmeriFlux network in the present study.

References

Alley, R., Berntsen, T., Bindoff, N.L., Chen, Z., Chidthaisong, A., Fridlingstein, P., Gregory, J., Hegerl, G., Heimann, M., Hewitson, B., Hoskins, B., Joos, F., Jouzel, J., Kattsov, V., Lohmann, U., Manning, M., Matsuno, T., Molina, M., Nicholls, N., Overpeck, J., Qin, D., Raga, G., Ramaswamy, V., Ren, J., Rusticucci, M., Solomon, S., Somerville, R., Stocker, T.F., Stoot, P., Stouffer, R.J., Whetton, P., Wood, R.A., Wratt, D., 2007. Climate change 2007: the physical science basis, summary for policy makers. Intergovern. Panel Clim. Change, 2–21.

Baldocchi, D., Falge, E., Gu, L., 2001. FLUXNET: a new tool to study the temporal and spatial variability of ecosystem scale carbon dioxide, water vapor, and energy flux densities. Bull. Am. Meteorol. Soc. 82, 2415–2434.
Baldocchi, D.D., 2003. Assessing the eddy covariance technique for evaluating carbon dioxide exchange rates of ecosystems: past, present, and future. Glob. Change Biol. 9, 479–492.
Boone, R.D., Nadelhoffer, K.J., Canary, J.D., Kaye, J.P., 1998. Roots exert a strong influence on the temperature sensitivity of soil respiration. Nature 396, 570–572.
Bowden, R.D., Nadelhoffer, K.J., Boone, R.D., Melillo, J.M., Garrison, J.B., 1993. Contributions of aboveground litter, belowground litter, and root respiration to total soil respiration in a temperate mixed hardwood forests. Can. J. Forest Res. 23, 1402–1407.
Buchmann, N., Schulze, E.D., 1999. Net CO_2 and H_2O fluxes of terrestrial ecosystems. Glob. Biogeochem. Cycles 13, 751–760.
Ceccato, P., Gobron, N., Flasse, S., Pinty, B., Tarantola, S., 2002. Designing a spectral index to estimate vegetation water content from remote sensing data. Remote Sens. Environ. 82, 188–207.
Clark, D.A., Brown, S., Kicklighter, D.W., Chambers, J.Q., Thomlinson, J.R., Ni, J., 2001. Measuring net primary production in forests: concepts and field methods. Ecol. Appl. 11, 356–370.
Cook, B.D., Davis, K.J., Wang, W., Desai, A.R., Berger, B.W., Teclaw, R.M., Martin, J.G., Bolstad, P.V., Bakwin, P.S., Yi, C., Heilman, W., 2004. Carbon exchange and venting anomalies in an upland deciduous forest in Northern Wisconsin, USA. Agric. Forest Meterol. 126, 271–295.
Curtis, P.S., Hanson, P.J., Bolstad, P., Barford, C., Randolph, J.C., Schmid, H.P., Wilson, K.B., 2002. Biometric and eddy-covariance based estimates of annual carbon storage in five eastern North American deciduous forests. Agric. Forest Meterol. 113, 3–19.
Desai, A.R., Bolstad, P.V., Cook, B.D., Davis, K.J., Carey, E.V., 2005. Comparing net ecosystem exchange of carbon dioxide between an old-growth and mature forest in the upper Midwest, USA. Agric. Forest Meterol. 128, 33–55.
Falge, E., Baldocchi, D., Olson, R.J., Anthoni, P., Aubinet, M., Bernhofer, C., Burba, G., Ceulemans, R., Clement, R., Dolman, H., Granier, A., Gross, P., Grunwald, T., Hollinger, D., Jensen, N.O., Katul, G., Keronen, P., Kowalski, A., Ta Lai, C., Law, B.E., Meyers, T., Moncrieff, J., Moors, E., Munger, J.W., Pilegaard, K., Rannik, U., Suyker, A., Tenhunen, J., Tu, K., Verma, S., Vesala, T., Wilson, K., Wofsy, S., 2001. Gap filling strategies for defensible annual sums of net ecosystem exchange. Agric. Forest Meterol. 107, 43–69.
Fensholt, R., Sandholt, I., 2003. Derivation of a shortwave infrared water stress index from MODIS near and shortwave infrared data in a semiarid environment. Remote Sens. Environ. 87, 111–121.
Gao, B.C., 1996. NDWI—a normalized difference water index for remote sensing of vegetation liquid water from space. Remote Sens. Environ. 58, 257–266.
Göckede, M., Foken, T., Aubinet, M., Aurela, M., Banaz, J., Bernhofer, C., Boonefond, J.M., Brunet, Y., Carrara, A., Clement, R., Dellwik, E., Elbers, J., Eugster, W., Fuhrer, J., Granier, A., Grünwald, T., Heinesch, B., Janssens, I.A., Knohl, A., Koeble, R., Laurila, T., Longdoz, B., Manca, G., Marek, M., Markkanen, T., Mateus, J., Matteucci, G., Mauder, M., Migliavacca, M., Minerbi, S., Moncrieff, J., Montagnani, L., Moors, E., Ourcival, J.M., Papale, D., Pereira, J., Pilegaard, K., Pita, G., Rambal, S., Rebmann, C., Rodrigues, A., Rotenberg, E., Sanz, M.J., Sedlak, P., Seufert, G., Siebicke, L., Soussana, J.F., Valentini, R., Verbeeck, H., Yakir, D., 2008. Quality control of CarboEurope flux data. Part 1. Coupling footprint analyses with flux data quality assessment to evaluate sites in forest ecosystems. Biogeosciences 5, 433–450.
Goldstein, A.H., Hultman, N.E., Fracheboud, J.M., Bauer, M.R., Panek, J.A., Xu, M., Qi, Y., Guenther, A.B., Baugh, W., 2000. Effects of climate variability on the carbon dioxide, water, and sensible heat fluxes above a ponderosa pine plantation in the Sierra Nevada (CA). Agric. Forest Meterol. 101, 113–129.
Gregory, P.A., George, V.N.P., Joseph, M., David, E.K., John, K.C., James, J., Ty, K.B., Aravindh, B., Guayana, P.A., Eloy, V., Laura, S., Michael, V., Hughes, R.F., 2010. High-resolution forest carbon stocks and emissions in the Amazon. PNAS 107, 16738–16742.
Hollinger, D.Y., Aber, J., Dail, B., Davidson, E.A., Goltz, S.M., Hughes, H., Leclerc, M.Y., Lee, J.T., Richardson, A.D., Rodrigues, C., Scott, N.A., Achuatavarier, D., Walsh, J., 2004. Spatial and temporal variability in forest-atmosphere CO_2 exchange. Glob. Change Biol. 10, 1689–1706.
Jackson, T.J., Chen, D., Cosh, M., Li, F., Anderson, M., Walthall, C., Doriaswamy, P., Hunt, E.R., 2004. Vegetation water content mapping using Landsat data derived normalized difference water index for corn and soybeans. Remote Sens. Environ. 92, 475–482.
Huete, A., Didan, K., Miura, T., Rodriguez, E.P., Gao, X., Ferreira, L.G., 2002. Overview of the radiometric and biophysical performance of the MODIS vegetation indices. Remote Sens. Environ. 83, 195–213.
Law, B.E., Falge, E., Gu, L., Baldocchi, D.D., Bakwin, P., Berbigier, P., Davis, K., Dolman, A.J., Falk, M., Fuentes, J.D., Goldstein, A., Granier, A., Grelle, A., Hollinger, D., Janssens, I.A., Jarvis, P., Jensen, N.O., Katul, G., Malhi, Y., Matteucci, G., Meyers, T., Monson, R., Munger, W., Oechel, W., Olson, R., Pilegaard, K., Paw, U.K.T., Thorgeirsson, H., Valentini, R., Verma, S., Vesala, T., Wilson, K., Wofsy, S., 2002. Environmental controls over carbon dioxide and water vapor exchange of terrestrial vegetation. Agric. Forest Meterol. 113, 97–120.
Li, Z.Q., Yu, G.R., Xiao, X.M., Li, Y.N., Zhao, X.Q., Ren, C.Y., Zhang, L.M., Fu, Y.L., 2007. Modeling gross primary production of alpine ecosystems in the Tibetan Plateau using MODIS images and climate data. Remote Sens. Environ. 107, 510–519.
Mahadevan, P., Wofsy, S.C., Matross, D.M., Xiao, X., Dunn, A.L., Lin, J.C., Gerbig, C., Munger, J.W., Chow, V.Y., Gottlieb, E.W., 2008. A satellite-based biosphere parameterization for net ecosystem CO_2 exchange: vegetation photosynthesis and respiration model (VPRM). Glob. Biogeochem. Cycles 22, 1–17.
Moffat, A.M., Papale, D., Reichstein, M., Hollinger, D.Y., Richardson, A.D., Barr, A.G., Beckstein, C., Braswell, B.H., Churkina, G., Desai, A.R., Falge, E., Gove, J.H., Heimann, M., Hui, D., Jarvis, A.J., Kattge, J., Noormets, A., Stauch, V.J., 2007. Comprehensive comparison of gap-filling techniques for eddy covariance net carbon fluxes. Agric. Forest Meterol. 147, 209–232.
Monson, R.K., Turnipseed, A.A., Sparks, J.P., Harley, P.C., Scott-Denton, L.E., Sparks, K., Huxman, T.E., 2002. Carbon sequestration in a high-elevation, subalpine forest. Glob. Change Biol. 8, 459–478.
Oren, R., Hsieh, C.L., Stoy, P., Albertson, J., McCarthy, H.R., Harrell, P., Katul, G.G., 2006. Estimating the uncertainty in annual net ecosystem carbon exchange: spatial variation in turbulent fluxes and sampling errors in eddy-covariance measurements. Glob. Change Biol. 12, 883–896.
Pacala, S.W., Hurtt, G.C., Baker, D., Peylin, P., Houghton, R.A., Birdsey, R.A., Heath, L., Sundquist, E.T., Stallard, R.F., Ciais, P., Moorcroft, P., Caspersen, J.P., Shevliakova, E., Moore, B., Kohlmaier, G., Holland, E., Gloor, M., Harmon, M.E., Fan, S.M., Sarmiento, J.L., Goodale, C.L., Schimel, D., Field, C.B., 2001. Consistent land and atmosphere-based U.S. carbon sink estimates. Science 292, 2316–2320.
Papale, D., Valentini, A., 2003. A new assessment of European forests carbon exchange by eddy fluxes and artificial neural network spatialization. Glob. Change Biol. 9, 525–535.
Powell, T.L., Bracho, R., Li, J.H., Dore, S., Hinkle, C.R., Drake, B.G., 2006. Environmental controls over net ecosystem carbon exchange of scrub oak in Central Florida. Agric. Forest Meterol. 141, 19–34.
Rahman, A.F., Sims, D.A., Cordova, V.D., Elmasri, B.Z., 2005. Potential of MODIS EVI and surface temperature for directly estimating per-pixel ecosystem C fluxes. Geophys. Res. Lett. 32, 194041–194046.
Reichstein, M., Falge, E., Baldocchi, D., Papale, D., Aubinet, M., Berbigier, P., Bernhofer, C., Buchmann, N., Gilmanov, T., Granier, A., Grunwald, T., Havrankova, K., Ilvesniemi, H., Janous, D., Knohl, A., Laurila, T., Lohila, A., Loustau, D., Matteucci, G., Meyers, T., Miglietta, F., Ourcival, J.M., Pumpanen, J., Rambal, S., Rotenberg, E., Sanz, M., Tenhunen, J., Seufert, G., Vaccari, F., Vesala, T., Yakir, D., Valentini, R., 2005. On the separation of net ecosystem exchange into assimilation and ecosystem respiration: review and improved algorithm. Glob. Change Biol. 11, 1424–1439.
Richardson, A.D., Mahecha, M.D., Falge, E., Kattge, J., Moffat, A.M., Papale, D., Reichstein, M., Stauch, V.J., Braswell, B.H., Churkina, G., Kruijt, B., Hollinger, D.Y., 2008. Statistical properties of random CO_2 flux measurement uncertainty inferred from model residuals. Agric. Forest Meterol. 148, 38–50.
Ruimy, A., Jarvis, P.G., Baldocchi, D.D., Saugier, B., 1996. CO_2 fluxes over plant canopies and solar radiation: a review. Adv. Ecol. Res. 26, 1–68.
Running, S.W., Nemani, R.R., Heinsch, F.A., Zhao, M., Reeves, M., Hashimoto, H., 2004. A continuous satellite-derived measure of global terrestrial primary production. Bioscience 54, 547–560.
Ryan, M.G., Law, B.E., 2005. Interpreting, measuring, and modeling soil respiration. Biogeochemistry 73, 3–27.
Schimel, D.S., 1995. Terrestrial ecosystems and the carbon cycle. Glob. Change Biol. 1, 77–91.
Schimel, D.S., House, J.I., Hibbard, K.A., Bousquet, P., Ciais, P., Peylin, P., Braswell, B.H., Apps, M.J., Baker, D., 2001. Recent patterns and mechanisms of carbon exchange by terrestrial ecosystems. Nature 414, 169–172.
Schmid, H.P., Grimmond, C.S.B., Cropley, F., Offerle, B., Su, H., 2000. Measurements of CO_2 and energy fluxes over a mixed hardwood forest in the mid-Western United States. Agric. Forest Meteorol. 103, 57–374.
Schubert, P., Eklundeh, L., Magnus, L., Nilsson, M., 2010. Estimating northern peatland CO_2 exchange from MODIS time series data. Remote Sens. Environ. 114, 1178–1189.
Schulze, E.D., Heimann, M., 1998. In: Galloway, J., Melillo, J. (Eds.), Asian Change in the Context of Global Change. University Press, Cambridge, UK, pp. 145–161.
Sims, D.A., Rahman, A.F., Vicente, D.C., 2008. A new model of gross primary productivity for North American ecosystems based solely on the enhanced vegetation index and land surface temperature from MODIS. Remote Sens. Environ. 112, 1633–1646.
Soccr, 2007. In: King, A.W., Dilling, L., Zimmerman, G.P., Fairman, D.M., Houghton, R.A., Marland, G.A., Rose, A.Z., Wilbanks, T.J. (Eds.), The First State of the Carbon Cycle Report (SOCCR). The North American Carbon Budget and Implications for the Global Carbon Cycle. US Climate Change Science Program, Washington, DC.
Tang, X.G., Liu, D.W., Song, K.S., Munger, J.W., Zhang, B., Wang, Z.M., 2011. A new model of net ecosystem carbon exchange for the deciduous-dominated forest by integrating MODIS and flux data. Ecol. Eng. 37, 1567–1571.
Thomas, C.K., Law, B.E., Irvine, J., Martin, J.G., Pettijohn, J.C., Davis, K.J., 2009. Seasonal hydrology explains interannual and seasonal variation in carbon and water exchange in a semiarid mature ponderosa pine forest in central Oregon. J. Geophys. Res. 114, 1–22.
Urbanski, S., Barford, C., Wofsy, C., Kucharik, C., Pyle, E., Budney, J., McKain, K., Fitzjarrald, D., Czikowsky, M., Munger, J.W., 2007. Factors controlling CO_2 exchange on time scales from hourly to decadal at Harvard forest. J. Geophys. Res. 112, 1–25.
Valentini, R., Matteucci, G., Dolman, A.J., Schulze, E.D., Rebmann, C., Moors, E.J., Granier, A., Gross, P., Jensen, N.O., Pilegaard, K., Lindroth, A., Grelle, A., Bernhofer, C., Grünwald, T., Aubinet, M., Ceulemans, R., Kowalski, A.S., Vesala, T., Rannik, Ü., Berbigier, P., Loustau, D., Guamundsson, J., Thorgeirsson, H., Ibrom, A., Morgenstern, K., Clement, R., Moncrieff, J., Montagnani, L., Minerbi, S., Jarvis,

P.G., 2000. Respiration as the main determinant of carbon balance in European forests. Nature 404, 861–865.

Wang, X., Jiang, Y.L., Jia, B.R., Wang, F.Y., Zhou, G.S., 2010. Comparison of soil respiration among three temperate forests in Changbai Mountains, China. Can. J. Forest Res. 40, 788–795.

Wu, C.Y., Munger, J.W., Niu, Z., Kuang, D., 2010. Comparison of multiple models for estimating gross primary production using MODIS and eddy covariance data in Harvard Forest. Remote Sens. Environ. 114, 2925–2939.

Wylie, B.K., Fosnight, E.A., Gilmanov, T.G., Frank, A.B., Morgan, J.A., Haferkamp, M.R., Meyers, T.P., 2007. Adaptive data-driven models for estimating carbon fluxes in the Northern Great Plains. Remote Sens. Environ. 106, 399–413.

Xiao, J., Zhuang, Q., Law, B.E., Chen, J., Baldocchi, D.D., Cook, D.R., Oren, R., Richardson, A.D., Wharton, S., Ma, S., Martin, T.A., Verma, S.B., Suyker, A.E., Scott, R.L., Monson, R.K., Litvak, M., Hollinger, D.Y., Sun, G., Davis, K.J., Bolstad, P.V., Burns, S.P., Curtis, P.S., Drake, B.G., Falk, M., Fischer, M.L., Foster, D.R., Gu, L., Hadley, J.L., Katul, G.G., Matamala, R., McNulty, S., Meyers, T.P., Munger, J.W., Noormets, A., Oechel, W.C., Paw, U.K.T., Schmid, H.P., Starr, G., Torn, M.S., Wofsy, S.C., 2010. A continuous measure of gross primary production for the conterminous U.S. derived from MODIS and AmeriFlux data. Remote Sens. Environ. 114, 576–591.

Xiao, J.F., Zhuang, Q.L., Law, B.E., Baldocchi, D.D., Chen, J.Q., Richardson, A.D., Melillo, J.M., Davis, K.J., Hollinger, D.Y., Wharton, S., Oren, R., Noormets, A., Fischer, M.L., Verma, S.B., Cook, D.R., Sun, G., McNulty, S., Wofsy, S.C., Bolstad, P.V., Burns, S.P., Curtis, P.S., Drake, B.G., Falk, M., Foster, D.R., Gu, L., Hadley, J.L., Katul, G.G., Litvak, M., Ma, S., Martin, T.A., Matamala, R., Meyers, T.P., Monson, R.K., Munger, J.W., Oechel, W.C., Paw, U.K.T., Schmid, H.P., Scott, R.L., Starr, G., Suyker, A.E., Torn, M.S., 2011. Assessing net ecosystem carbon exchange of U.S. terrestrial ecosystems by integrating eddy covariance flux measurements and satellite observations. Agric. Forest Meterol. 151, 60–69.

Xiao, X.M., Zhang, Q.Y., Hollinger, D., Aber, J., Moore, I.B., 2005. Modeling gross primary production of an evergreen needleleaf forest using MODIS and climate data. Ecol. Appl. 15, 954–969.

Yamaji, T., Sakai, T., Endo, T., Baruah, P.J., Akiyama, T., Saigusa, N., Nakai, Y., Kitamura, K., Ishizuka, M., Yasuoka, Y., 2008. Scaling-up technique for net ecosystem productivity of deciduous broadleaved forests in Japan using MODIS data. Ecol. Res. 23, 765–775.

Yuan, J.G., Niu, Z., Wang, C.L., 2006. Vegetation NPP distribution based on MODIS data and CASA model—a case study of Northern Hebei Province. Chin. Geogr. Sci. 16, 334–341.

Zhang, M., Yu, G.R., Zhang, L.M., Sun, X.M., Wen, X.F., Han, S.J., 2009. Effects of solar radiation on net ecosystem exchange of broadleaved-Korean Pine mixed forest in Changbai Mountain. Chin. J. Plant Ecol. 33, 270–282.

Zhou, L.Y., Jia, B.R., Zhou, G.S., Zeng, W., Wang, Y., 2010. Carbon exchange of Chinese boreal forest during its growth season and related regulation mechanisms. Chin. J. Appl. Ecol. 21, 2449–2456.

Zhu, B., Wang, X.P., Fang, J.Y., Piao, S.L., Shen, H.H., Zhao, S.Q., Peng, C.H., 2010. Altitudinal changes in carbon storage of temperate forests on Mt Changbai, Northeast China. J. Plant Res. 123, 439–452.